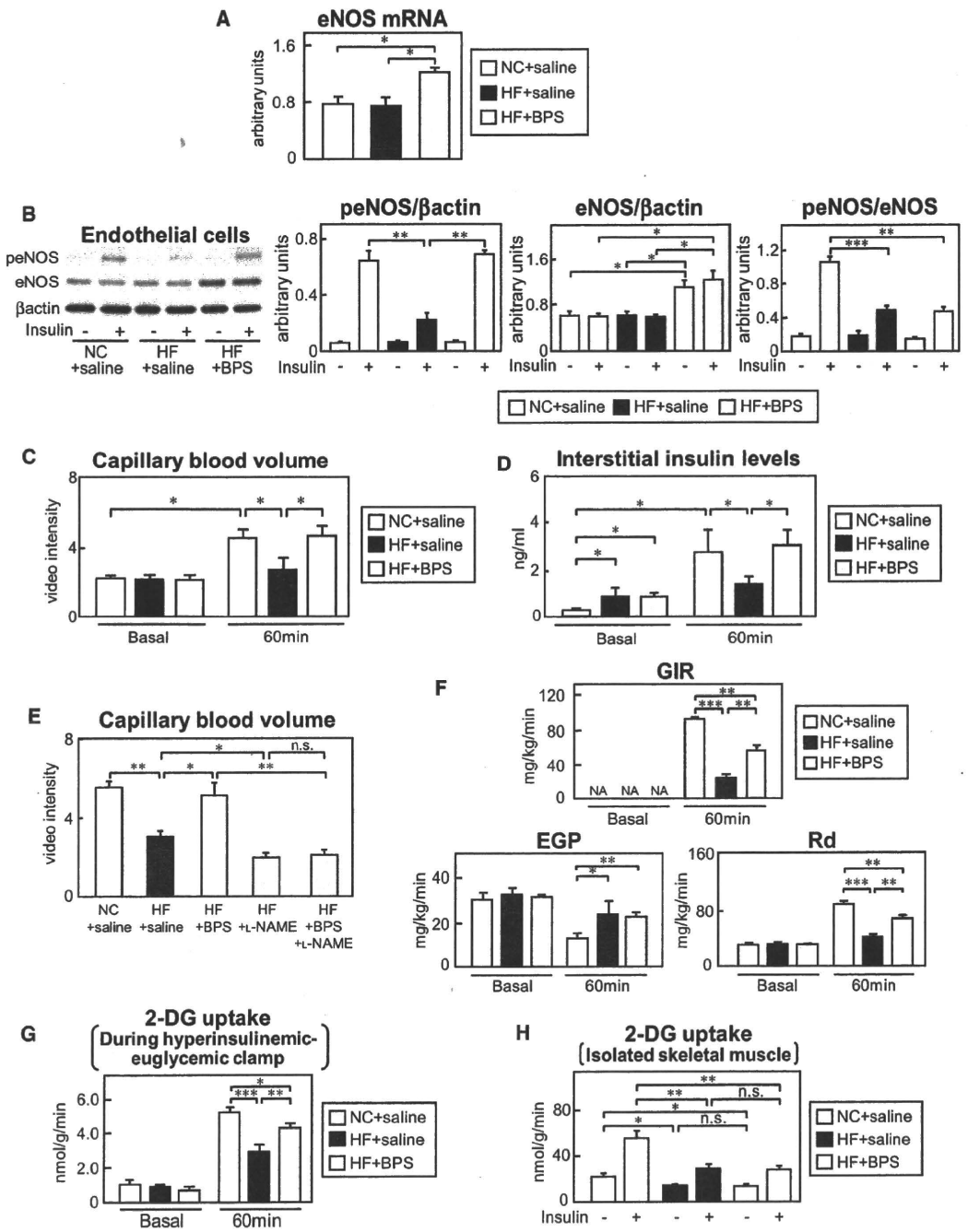

Figure 5. Restoration of the Insulin-Induced Phosphorylation of eNOS Restored the Insulin-Induced Increase of the Capillary Blood Volume and Interstitial Insulin Concentrations, Resulting in Improvement of the Glucose Uptake by the Skeletal Muscle in the HF Diet-Fed Obese Mice

(A–D) eNOS mRNA levels in the endothelial cells (A), insulin-stimulated phosphorylation level of eNOS (B), capillary blood volume (C), and interstitial insulin concentrations (D) in the BPS-treated HF diet-fed mice (n = 5–8).

(E) Capillary blood volume in the BPS-treated HF diet-fed mice following L-NAME treatment (n = 4–6).

(F) GIR, EGP, and Rd in the BPS-treated HF diet-fed mice after insulin infusion in the hyperinsulinemic-euglycemic clamp study (n = 3–5).

(G) Glucose uptake by the skeletal muscle in the BPS-treated HF diet-fed mice after insulin infusion in the hyperinsulinemic-euglycemic clamp study (n = 3–5).

(H) Glucose uptake by the isolated skeletal muscle in the BPS-treated HF diet-fed mice (n = 3–5). "NC" indicates normal chow-fed mice. "NA" indicates not applicable. Where error bars are shown, the results represent the means ± SEM. *$p < 0.05$, **$p < 0.01$, ***$p < 0.001$.

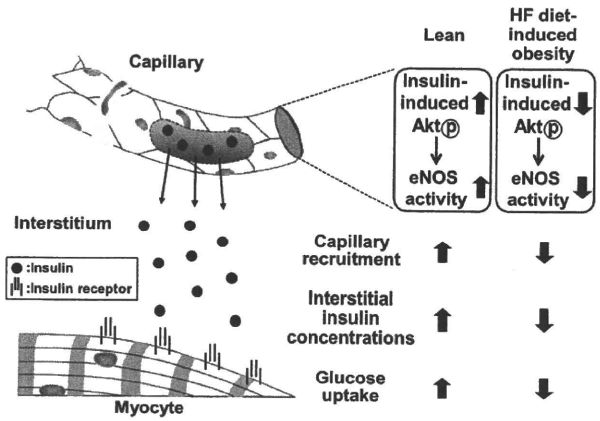

Figure 6. Impaired Insulin Signaling in the Endothelial Cells Reduces Insulin-Induced Glucose Uptake by the Skeletal Muscle in Obese Subjects

In lean subjects, the insulin-mediated Akt and eNOS activations are induced optimally in the endothelial cells after feeding, resulting in insulin-induced capillary recruitment, increase of interstitial insulin concentrations, and increase of the glucose uptake by the skeletal muscle. By contrast, since the insulin-mediated Akt and eNOS activations are inadequate in the endothelial cells of obese subjects after feeding, the insulin-induced capillary recruitment, increase or interstitial insulin concentrations, and increase of glucose uptake by the skeletal muscle are impaired.

Moreover, insulin delivery into the interstitial fluid is known to be delayed in insulin resistance (Sjostrand et al., 2002), as also is the onset of insulin stimulation of glucose uptake (Nolan et al., 1997). In addition, delivery of inulin, a molecule whose molecular weight is similar to that of insulin, to the skeletal muscle was reported to be markedly diminished in diet-induced insulin resistance (Ellmerer et al., 2006). These findings suggest that impairment of insulin delivery, possibly caused by an endothelial insulin signaling defect, may play a critical role in the skeletal muscle insulin resistance seen in obesity.

Why were decreased insulin signaling and decreased glucose uptake in response to insulin observed only in the skeletal muscle of the ETIrs2KO mice and not in their liver? The difference between the types of capillaries in the liver and skeletal muscle may explain these differences in the insulin sensitivity of the two organs. It is thought that the occluded junctions of the endothelial cells of the capillaries in the skeletal muscle may prevent paracellular transport of most macromolecules, including insulin, whereas the fenestrated endothelium of the capillaries in the liver freely permits paracellular passage of macromolecules (Aird, 2007). In fact, more rapid insulin action kinetics have been observed in the liver than in the skeletal muscle (Sherwin et al., 1974).

Insulin-induced phosphorylation of Akt and eNOS in the ETIrs2KO mice was significantly, but not completely, impaired by endothelial Irs2 deficiency (Figure 2D), suggesting the important role of both Irs2 and Irs1 in this signaling in the endothelial cells. In fact, phosphorylation of Akt and eNOS was completely abrogated in the ETIrs1/2DKO mice (Figure 3I). Thus, in the physiological state, it is likely that insulin-stimulated Irs1-mediated Akt activates eNOS in proportion to the amount of eNOS protein available in these mice.

In this study, we found that endothelial insulin signaling mediates insulin-stimulated capillary recruitment and increase of interstitial insulin concentrations and, as a consequence, facilitates glucose uptake by the skeletal muscle. Skeletal muscle insulin resistance may be caused by impaired insulin signaling not only in the myocytes but also in the endothelial cells. Taken together, treatment directed at improving insulin signaling in the endothelial cells as well as myocytes may serve as a therapeutic strategy for ameliorating skeletal muscle insulin resistance.

EXPERIMENTAL PROCEDURES

Mice

ETIrs1KO or ETIrs2KO mice were generated by mating $Irs1^{lox/+}$ or $Irs2^{lox/+}$ female mice (Kubota et al., 2008) with transgenic mice expressing Cre under control of the murine Tie2 promoter (Tie2-Cre mice) (Kisanuki et al., 2001). The $Irs1^{lox/+}$:Tie2-Cre or $Irs2^{lox/+}$:Tie2-Cre male offspring were then crossed with $Irs1^{lox/+}$ or $Irs2^{lox/+}$ female mice to obtain WT ($Irs1^{+/+}$), Tie2-Cre ($Irs1^{+/+}$:Tie2-Cre), control ($Irs1^{lox/lox}$), and ETIrs1KO ($Irs1^{lox/lox}$:Tie2-Cre) mice, or WT ($Irs2^{+/+}$), Tie2-Cre ($Irs2^{+/+}$:Tie2-Cre), control ($Irs2^{lox/lox}$), and ETIrs2KO ($Irs2^{lox/lox}$:Tie2-Cre) mice, respectively. To generate endothelial-specific Irs1/Irs2 double-knockout (ETIrs1/2DKO) mice, $Irs1^{lox/+}$:Tie2-Cre or $Irs2^{lox/+}$:Tie2-Cre male mice were crossed with $Irs2^{lox/+}$ or $Irs1^{lox/+}$ female mice, and the resultant $Irs1^{lox/+}/Irs2^{lox/+}$:Tie2-Cre male mice were crossed with $Irs1^{lox/+}/Irs2^{lox/+}$ female mice. $Irs1^{lox/lox}/Irs2^{lox/lox}$ mice were used as the control for ETIrs1/2DKO mice. Only male littermates were used for this study; we did not use the female Tie2-Cre, $Irs1^{lox/+}$:Tie2-Cre, $Irs2^{lox/+}$:Tie2-Cre, $Irs1^{lox/+}/Irs2^{lox/+}$:Tie2-Cre, ETIrs1KO, ETIrs2KO, or ETIrs1/2DKO mice for breeding. Further information is provided in the Supplemental Information. The animal care and experimental procedures used in this study were approved by the Animal Care Committee of the University of Tokyo.

Capillary Blood Volume

The capillary blood volume was measured by contrast-enhanced ultrasound, as described previously (Vincent et al., 2004), with some modifications. The hindlimb muscles were imaged in the short axis using a 40 MHz transducer (RMV 704) connected to an ultrasound system (Vevo 770; VISUALSONICS Inc.). Sonazoid (Daiichi Sankyo Corporation) was infused into the animals, which were divided into three groups for the measurements at 0, 10, and 60 min after the hyperinsulinemic-euglycemic clamp, a high-power ultrasound with a frequency of 1MHz was applied to the lower leg muscles, and images were collected for 30 s to assess the enhancement. The ultrasound intensity in decibels within the region of interest was converted to the acoustic intensity after background subtraction using 0.5 s ultrasound images, and the microvascular volume, fill rate constant, and capillary blood volume were calculated according to the equation $y = A(1 - e^{-\beta t})$. Further information is provided in the Supplemental Information.

Interstitial Concentrations of Insulin in the Skeletal Muscle

Muscle microdialysis was performed in the hindlimb muscles using a 4 mm microdialysis tubing (CMA-20) at the rate of 0.3 μl/min. We conducted calibration using the no-net flux technique described previously (Jansson et al., 1993), with slight modifications. Briefly, four known concentrations of insulin (0 ng/ml, 0.5 ng/ml, 1 ng/ml, and 1.5 ng/ml) above and below the expected concentration in the skeletal muscle were used. The insulin solutions were added to the perfusate, and the net changes in the concentrations of the analytes in the dialysate were recorded ($insulin_{out} - insulin_{in}$ = net change). Regression analysis yielded a linear relationship between the concentrations in the perfusates and the dialysates. The intercept with the x axis indicates the insulin concentrations in the perfusate at equilibrium with the surrounding medium, and the slope of the line yields the dialysis recovery by the no-net flux technique. The insulin concentrations in the interstitial fluid were calculated from the dialysis recovery by the no-net flux technique and the in vivo dialysate insulin concentration, as described previously (Sjostrand et al., 2002).

Endothelial Cell Culture

The aorta was dissected out from the aortic arch to the abdominal aorta and immersed in 10% FBS-DMEM containing 1000 U/ml heparin. A 24-gauge cannula was inserted into the proximal portion of the aorta. The other side was tied, and the lumen was filled with a solution of collagenase type II (2 mg/ml, dissolved in serum-free DMEM). After incubation at 37°C for 45 min, the endothelial cells were removed from the aorta by flushing with 5 ml of DMEM containing 10% FBS and cultured in a 35 mm collagen type 1-coated dish. Further information is provided in the Supplemental Information.

Hyperinsulinemic-Euglycemic Clamp

An infusion catheter was inserted into the right jugular vein of the mice, as described previously (Kubota et al., 2008), with some modifications. 1% glucose ([6,6-$^2H_2$]glucose [Sigma]) was infused intravenously, and after a 90 min basal period a blood sample was collected from the tail tip for determination of the basal glucose specific activity. To measure the GIR, a primed-continuous infusion of insulin (Humulin R; Lilly) was administered and the blood glucose concentration was maintained at approximately 120 mg/dl by the administration of glucose (5 g of glucose/10 ml enriched to about 20% with [6,6-$^2H_2$]glucose [Sigma]) for 60 or 120 min. Blood samples (20 μl) were obtained for 15 or 30 min before the end of the hyperinsulinemic-euglycemic clamp. Thereafter, the Rd was calculated according to non-steady-state equations, and the EGP was calculated as the difference between the Rd values and the exogenous GIR. Further information is provided in the Supplemental Information.

Statistical Analysis

Values were expressed as means ± SEM. Student's t test was used for statistical analysis of the differences between two groups, and the statistical significance of differences among multiple groups was determined by ANOVA.

SUPPLEMENTAL INFORMATION

Supplemental Information includes six figures, one movie, Supplemental Experimental Procedures, and Supplemental References and can be found with this article at doi:10.1016/j.cmet.2011.01.018.

ACKNOWLEDGMENTS

We thank Namiko Okajima-Kasuga, Sayaka Sasamoto, Kousuke Yokota, Miyoko Suzuki-Nakazawa, Masahiro Nakamaru, Michiko Kato, Tomoko Asano, Eishin Hirata, Eri Yoshida-Nagata, Ayumi Nagano, Miharu Nakashima, Ritsuko Fujita, and Hiroshi Chiyonobu for their technical assistance and care of the animals. This work was supported by a grant for CREST from the Japan Science and Technology Corporation; a grant for Promotion of Fundamental Studies in Health Science from the Organization for Pharmaceutical Safety and Research; a grant for TSBMI from the Ministry of Education, Culture, Sports, Science and Technology of Japan; a Grant-in-Aid for Scientific Research in Priority Areas (A) (16209030), (A) (18209033), and (S) (20229008) from the Ministry of Education, Culture, Sports, Science, and Technology of Japan (to T. Kadowaki); and a Grant-in-Aid for Scientific Research in Priority Areas (C) (19591037) and (B) (21390279) from the Ministry of Education, Culture, Sports, Science, and Technology of Japan (to N.K.).

Received: May 10, 2010
Revised: August 13, 2010
Accepted: January 24, 2011
Published: March 1, 2011

REFERENCES

Aird, W.C. (2007). Phenotypic heterogeneity of the endothelium. I. Structure, function, and mechanisms. Circ. Res. *100*, 158–173.

Barrett, E.J., Eggleston, E.M., Inyard, A.C., Wang, H., Li, G., Chai, W., and Liu, Z. (2009). The vascular actions of insulin control its delivery to muscle and regulate the rate-limiting step in skeletal muscle insulin action. Diabetologia *52*, 752–764.

Bergman, R.N. (1989). Lilly Lecture: toward physiological understanding of glucose tolerance: minimal-model approach. Diabetes *38*, 1512–1527.

Brüning, J.C., Michael, M.D., Winnary, J.N., Hayashi, T., Hörsch, D., Accili, D., Goodyear, L.J., and Kahn, C.R. (1998). A muscle-specific insulin receptor knockout exhibits features of the metabolic syndrome of NIDDM without altering glucose tolerance. Mol. Cell *2*, 559–569.

Chiu, J.D., Richey, J.M., Harrison, L.N., Zuniga, E., Kolk, C.M., Kirkman, E., Ellmerer, M., and Bergman, R.N. (2008). Direct administration of insulin into skeletal muscle reveals that the transport of insulin across the capillary endothelium limits the time course of insulin to activate glucose disposal. Diabetes *57*, 828–835.

Clark, M.G. (2008). Impaired microvascular perfusion: a consequence of vascular dysfunction and a potential cause of insulin resistance in muscle. Am. J. Physiol. Endocrinol. Metab. *295*, E732–E750.

DeFronzo, R.A., Tobin, J.D., and Andres, R. (1979). Glucose clamp technique: a method for quantifying insulin secretion and resistance. Am. J. Physiol. *237*, E214–E223.

Ellmerer, M., Hamilton-Wessler, M., Kim, S.P., Huecking, K., Kirkman, E., Chiu, J., Richey, J., and Bergman, R.N. (2006). Reduced access to insulin-sensitive tissues in dogs with obesity secondary to increased fat intake. Diabetes *55*, 1769–1775.

Hamilton-Wessler, M., Ader, M., Dea, M.K., Moore, D., Loftager, M., Markussen, J., and Bergman, R.N. (2002). Mode of transcapillary transport of insulin and insulin analog NN304 in dog hindlimb: evidence for passive diffusion. Diabetes *51*, 574–582.

Jansson, P.A., Fowelin, J.P., von Schenck, H.P., Smith, U.P., and Lönnroth, P.N. (1993). Measurement by microdialysis of the insulin concentration in subcutaneous interstitial fluid. Importance of the endothelial barrier for insulin. Diabetes *42*, 1469–1473.

Jiang, Z.Y., Lin, Y.W., Clemont, A., Feener, E.P., Hein, K.D., Igarashi, M., Yamauchi, T., White, M.F., and King, G.L. (1999). Characterization of selective resistance to insulin signaling in the vasculature of obese Zucker (fa/fa) rats. J. Clin. Invest. *104*, 447–457.

Kainoh, M., Maruyama, I., Nishio, S., and Nakadate, T. (1991). Enhancement by beraprost sodium, a stable analogue of prostacyclin, in thrombomodulin expression on membrane surface of cultured vascular endothelial cells via increase in cyclic AMP level. Biochem. Pharmacol. *41*, 1135–1140.

Karnieli, E., Zarnowski, M.J., Hissin, P.J., Simpson, I.A., Salans, L.B., and Cushman, S.W. (1981). Insulin-stimulated translocation of glucose transport systems in the isolated rat adipose cell. Time course, reversal, insulin concentration dependency, and relationship to glucose transport activity. J. Biol. Chem. *256*, 4772–4777.

Keske, M.A., Clerk, L.H., Price, W.J., Jahn, L.A., and Barrett, E.J. (2009). Obesity blunts microvascular recruitment in human forearm muscle after a mixed meal. Diabetes Care *32*, 1672–1677.

Kisanuki, Y.Y., Hammer, R.E., Miyazaki, J., Williams, S.C., Richardson, J.A., and Yanagisawa, M. (2001). Tie2-Cre transgenic mice: a new model for endothelial cell-lineage analysis in vivo. Dev. Biol. *230*, 230–242.

Kubota, T., Kubota, N., Moroi, M., Terauchi, Y., Kobayashi, T., Kamata, K., Suzuki, R., Tobe, K., Namiki, A., Aizawa, S., et al. (2003). Lack of insulin receptor substrate-2 causes progressive neointima formation in response to vessel injury. Circulation *107*, 3073–3080.

Kubota, N., Kubota, T., Itoh, S., Kumagai, H., Kozono, H., Takamoto, I., Mineyama, T., Ogata, H., Tokuyama, K., Ohsugi, M., et al. (2008). Dynamic functional relay between insulin receptor substrate 1 and 2 in hepatic insulin signaling during fasting and feeding. Cell Metab. *8*, 49–64.

Long, Y.C., and Zierath, J.R. (2008). Influence of AMP-activated protein kinase and calcineurin on metabolic networks in skeletal muscle. Am. J. Physiol. Endocrinol. Metab. *295*, E545–E552.

Miles, P.D., Levisetti, M., Reichart, D., Khoursheed, M., Moossa, A.R., and Olefsky, J.M. (1995). Kinetics of insulin action in vivo. Identification of rate limiting steps. Diabetes *44*, 947–953.

Muniyappa, R., and Quon, M.J. (2007). Insulin action and insulin resistance in vascular endothelium. Curr. Opin. Clin. Nutr. Metab. Care *10*, 523–530.

Niwano, K., Arai, M., Tomaru, K., Uchiyama, T., Ohyama, Y., and Kurabayashi, M. (2003). Transcriptional stimulation of the eNOS gene by the stable prostacyclin analogue beraprost is mediated through cAMP-responsive element in vascular endothelial cells: close link between PGI2 signal and NO pathways. Circ. Res. *93*, 523–530.

Nolan, J.J., Ludvik, B., Baloga, J., Reichart, D., and Olefsky, J.M. (1997). Mechanisms of the kinetic defect in insulin action in obesity and NIDDM. Diabetes *46*, 994–1000.

Petersen, K.F., Dufour, S., Befroy, D., Garcia, R., and Shulman, G.I. (2004). Impaired mitochondrial activity in the insulin-resistant offspring of patients with type 2 diabetes. N. Engl. J. Med. *350*, 664–671.

Rattigan, S., Clark, M.G., and Barrett, E.J. (1997). Hemodynamic actions of insulin in rat skeletal muscle: evidence for capillary recruitment. Diabetes *46*, 1381–1388.

Sherwin, R.S., Kramer, K.J., Tobin, J.D., Insel, P.A., Liljenquist, J.E., Berman, M., and Andres, R. (1974). A model of the kinetics of insulin in man. J. Clin. Invest. *53*, 1481–1492.

Sjostrand, M., Gudbjornsdottir, S., Holmang, A., Lonn, L., Strindberg, L., and Lönnroth, P. (2002). Delayed transcapillary transport of insulin to muscle interstitial fluid in obese subjects. Diabetes *51*, 2742–2748.

Vicent, D., Ilany, J., Kondo, T., Naruse, K., Fisher, S.J., Kisanuki, Y.Y., Bursell, S., Yanagisawa, M., King, G.L., and Kahn, C.R. (2003). The role of endothelial insulin signaling in the regulation of vascular tone and insulin resistance. J. Clin. Invest. *111*, 1373–1380.

Vincent, M.A., Clerk, L.H., Lindner, J.R., Klibanov, A.L., Clark, M.G., Rattigan, S., and Barrett, E.J. (2004). Microvascular recruitment is an early insulin effect that regulates skeletal muscle glucose uptake in vivo. Diabetes *53*, 1418–1423.

Vincent, M.A., Clerk, L.H., Rattigan, S., Clark, M.G., and Barrett, E.J. (2005). Active role for the vasculature in the delivery of insulin to skeletal muscle. Clin. Exp. Pharmacol. Physiol. *32*, 302–307.

Wallis, M.G., Wheatley, C.M., Rattigan, S., Barrett, E.J., Clark, A.D.H., and Clark, M.G. (2002). Insulin-mediated hemodynamic changes are impaired in muscle of Zucker obese rats. Diabetes *51*, 3492–3498.

Wang, H., Wang, A.X., Liu, Z., and Barrett, E.J. (2008). Insulin signaling stimulates insulin transport by bovine aortic endothelial cells. Diabetes *57*, 540–547.

White, M.F., and Kahn, C.R. (1994). The insulin signaling system. J. Biol. Chem. *269*, 1–4.

Yang, Y.J., Hope, I.D., Ader, M., and Bergman, R.N. (1989). Insulin transport across capillaries is rate limiting for insulin action in dogs. J. Clin. Invest. *84*, 1620–1628.